Tidal propagation in the Gulf of Khambhat, Bombay High, and surrounding areas

A S UNNIKRISHNAN, S R SHETYE and G S MICHAEL

National Institute of Oceanography, Dona-Paula, Goa 403 004, India.

The continental shelf on the west coast of India is widest off Bombay and leads into a strongly converging channel, the Gulf of Khambhat. Tides in the Gulf are among the largest on the coast. We use data on amplitude and phase of major semi-diurnal and diurnal constituents at forty-two ports in the Gulf and surrounding areas to define characteristics of the tides. We then use a barotropic numerical model based on shallow water wave equations to simulate the sea level and circulation in the region. The model is forced by prescribing the tide along the open boundaries of the model domain. Observed sea level at Bombay and currents from the Bombay High region at the centre of the model domain and from a shallow station off the port of Dahanu compare favourably with the fields simulated by the model. The simulated amplitudes and phases of the four most prominent tidal constituents also compare favourably with those observed along the coast, except at a few locations where the model spatial resolution (6.37 km × 6.37 km) appears to be inadequate to resolve the local geometry. Though this encourages us to conclude that the circulation in the region is dominated by barotropic tides, a concern is that the observational database on hydrography and directly measured currents in the region is weak.

1. Introduction

Width of the continental shelf on the west coast of India varies considerably from south to north. The shelf break on this coast is approximately along the 200 m depth contour. The distance between the coastline and the shelf break is about 50 km near the southern end of the coast at 8°N. The width increases to about 100 km off Malvan (16°N). Farther north, the shelf widens more rapidly and is over 250 km wide at about 19°N. It then gets narrower, and is about 100 km wide at 21°N. Located in the middle of the widest part of the shelf, at depths of a little more than 50 m, is the Bombay High oil field. Northeast of the oil field is the Gulf of Khambhat, a strongly converging channel (figure 1).

The region consisting of the wide shelf, including the Bombay High and the Gulf of Khambhat, is of interest for several reasons. The Gulf experiences tidal amplitudes that are amongst the largest observed on the west coast. Mumbai is located on the southeastern corner of the region. Industrial effluents and domestic sewage from the highly developed metropolitan area of this city enters the shelf in the region. India's largest offshore oil-field, the Bombay High, is located at the centre of the region (figure 1). A pipeline carries the crude oil from the offshore field to refineries near Mumbai. Finally, a number of major and minor ports line the coastline of the region. Many of the ports cater to fishing which is an important activity in the region. In short, the region is of considerable economic importance; equally important are concerns about its environment.

Industrial activity must be exerting considerable stress on the environment of the region continually. Such activity also carries with it potential for episodic events, such as accidents with serious implications to the environment. Another source for episodic disturbances on the environment are natural disasters. An example of this are cyclonic storms which are not uncommon in the region. All these considerations imply that environmental management is necessary in the region. An important component of such management is knowledge of the circulation of water in the region.

Keywords. Tidal constituents; tidal circulation; Bombay High; Gulf of Khambhat.

Proc. Indian Acad. Sci. (Earth Planet. Sci.), **108**, No. 3, September 1999, pp. 155–177

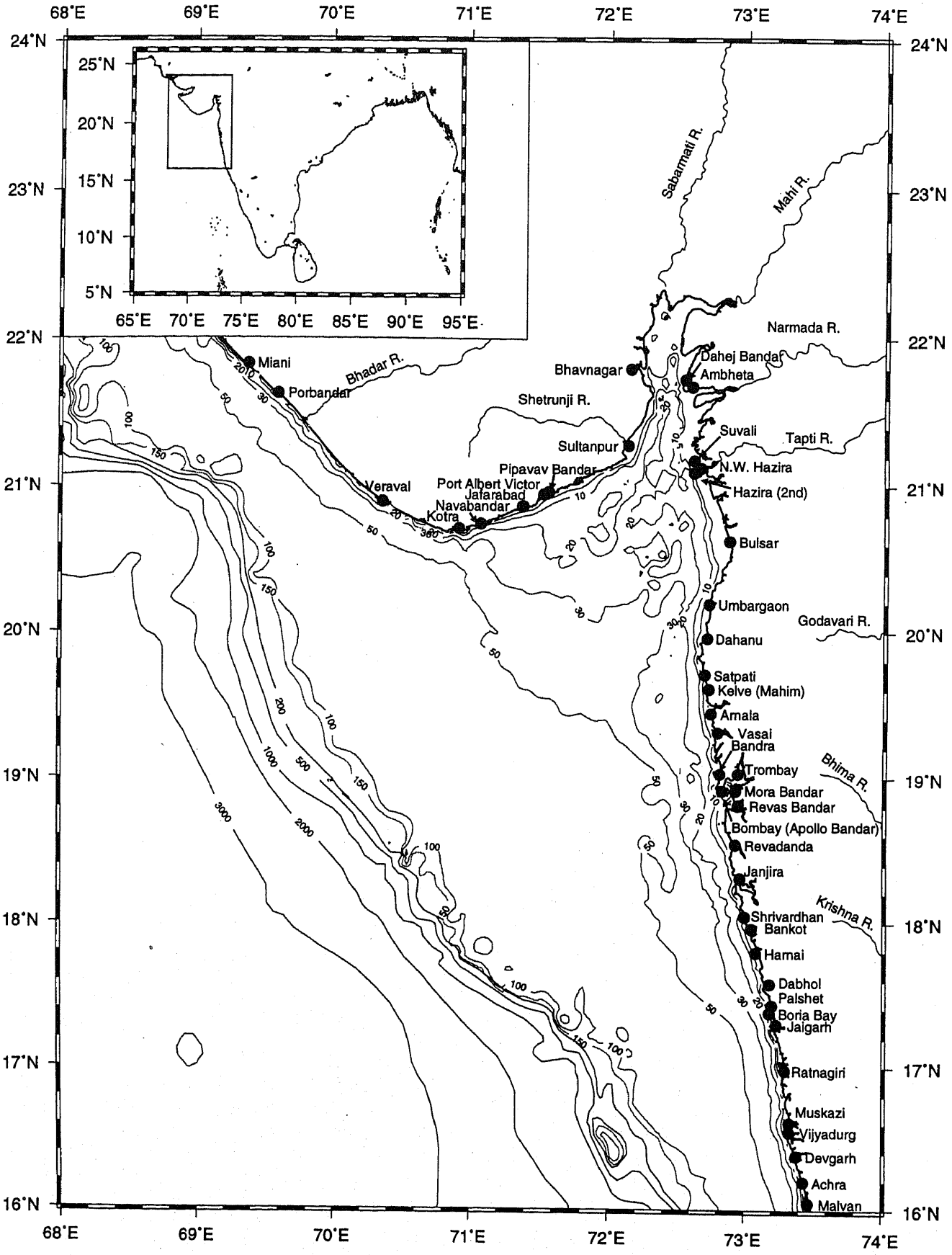

Figure 1. A map of the Gulf of Khambhat, Bombay High and surrounding areas. Depth contours are in metres. Data from 41 locations marked with circles have been used in figures 2–7.

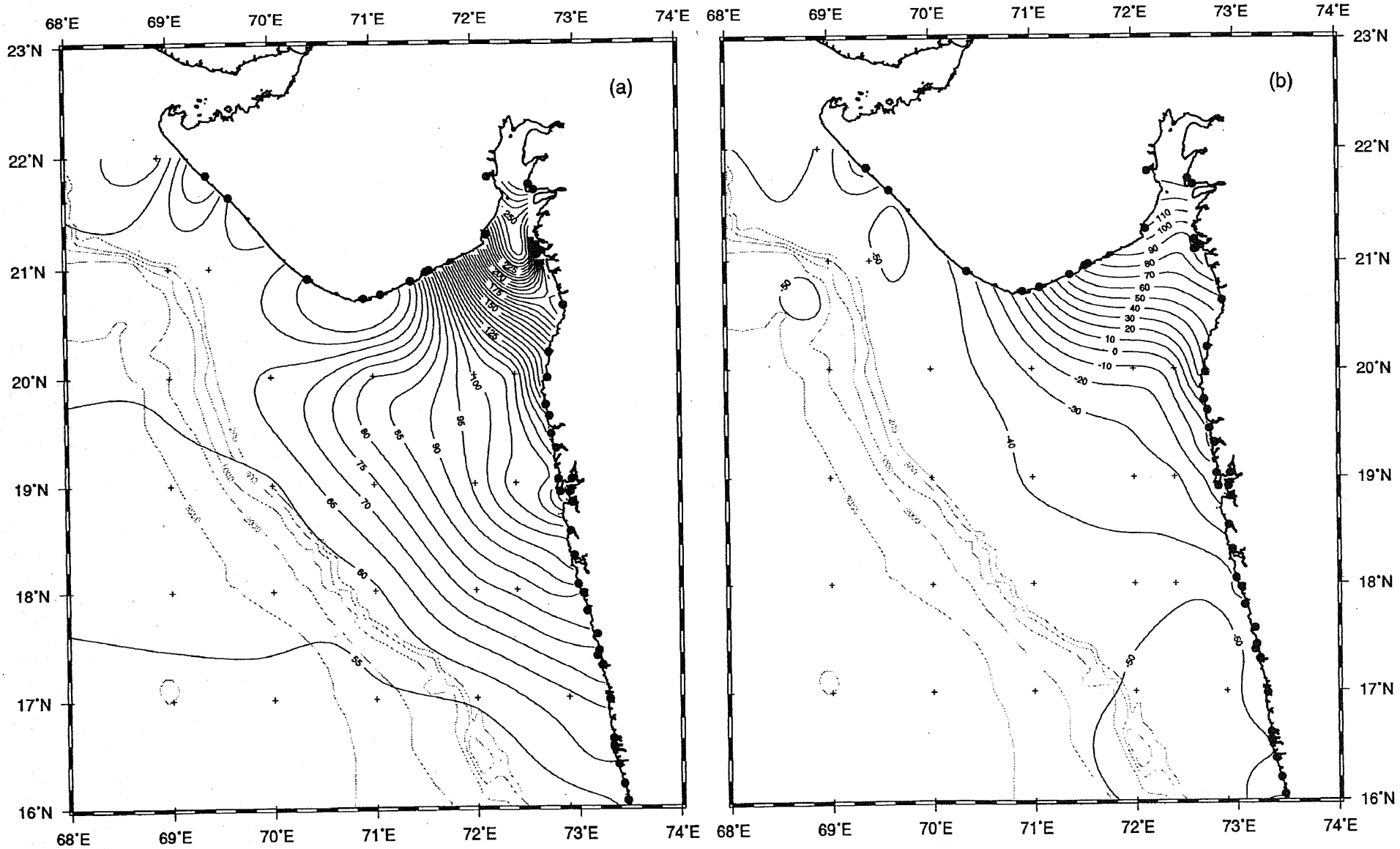

Figure 2. (a) Amplitude (cm) and (b) phase (degrees) of tidal constituent M_2.

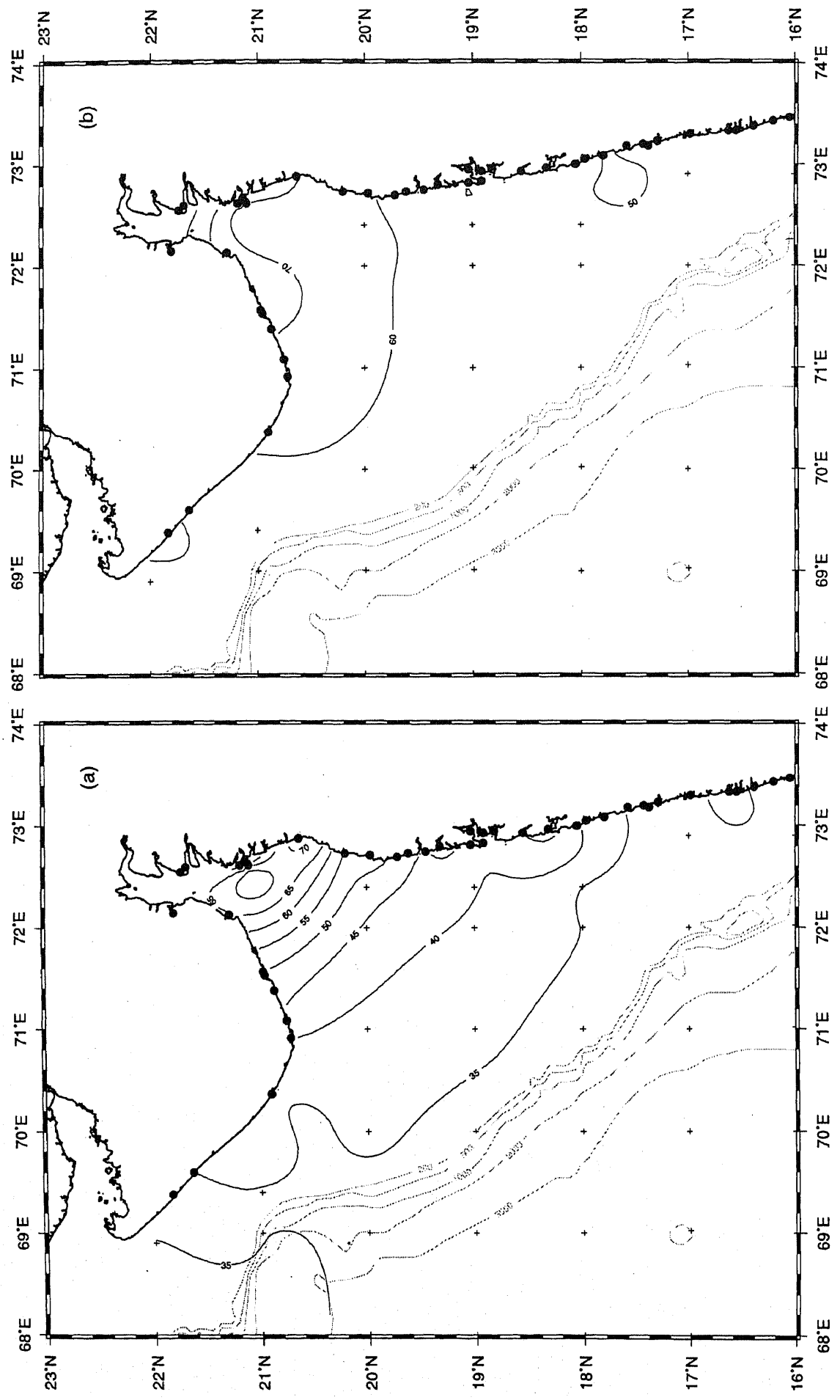

Figure 3. Same as figure 2, but for K_1.

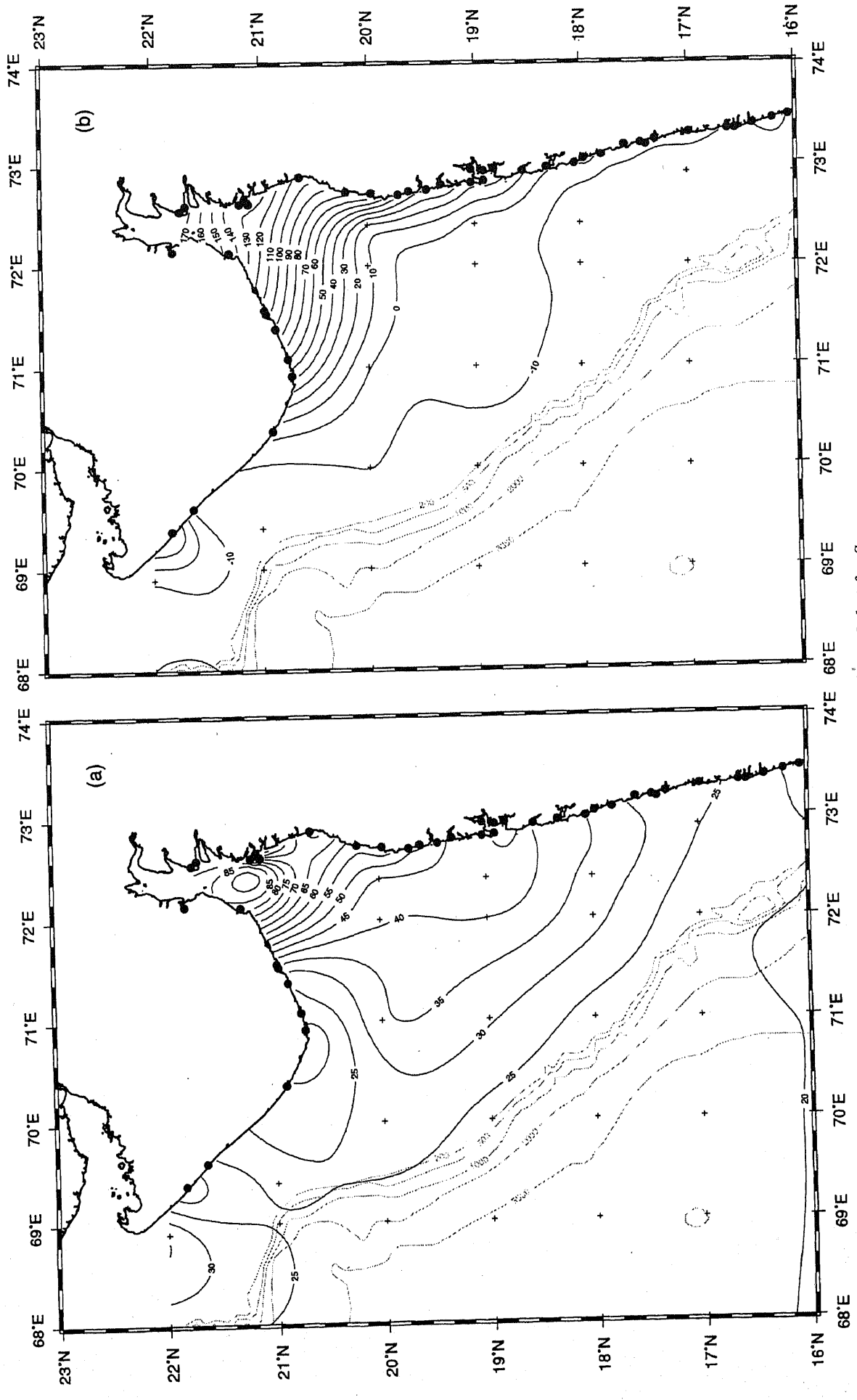

Figure 4. Same as figure 2, but for S_2.

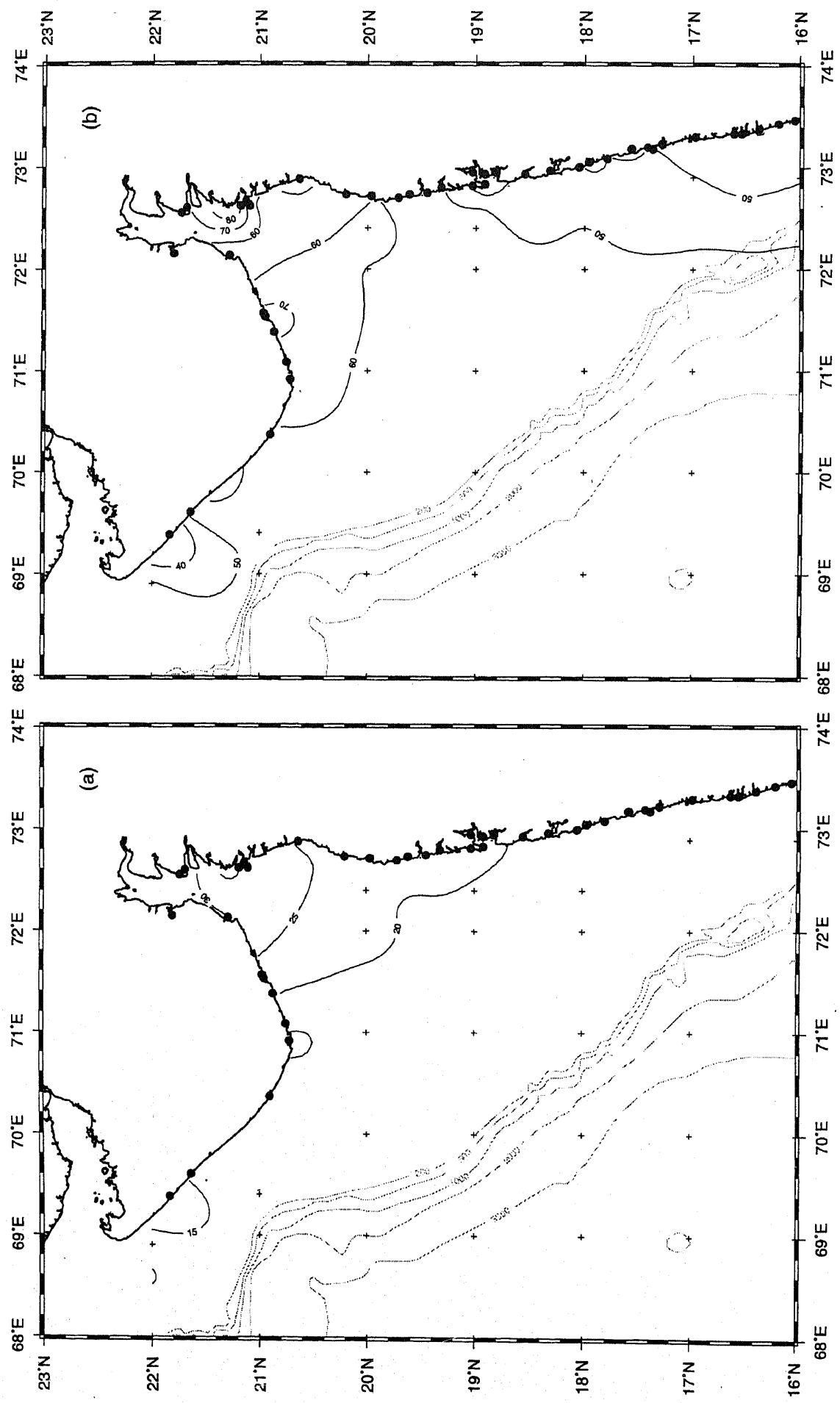

Figure 5. Same as figure 2, but for O_1.

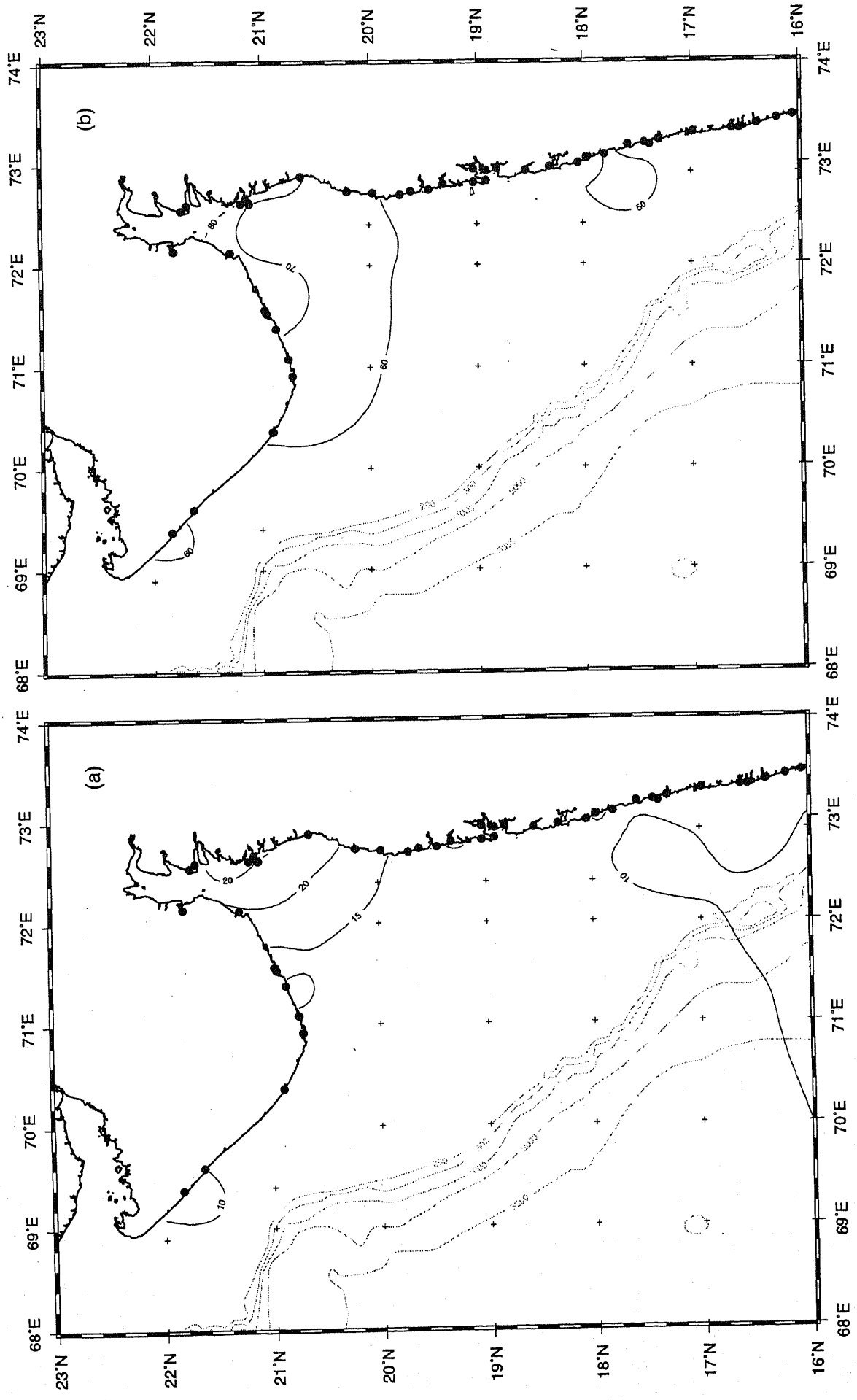

Figure 6. Same as figure 2, but for P_1.

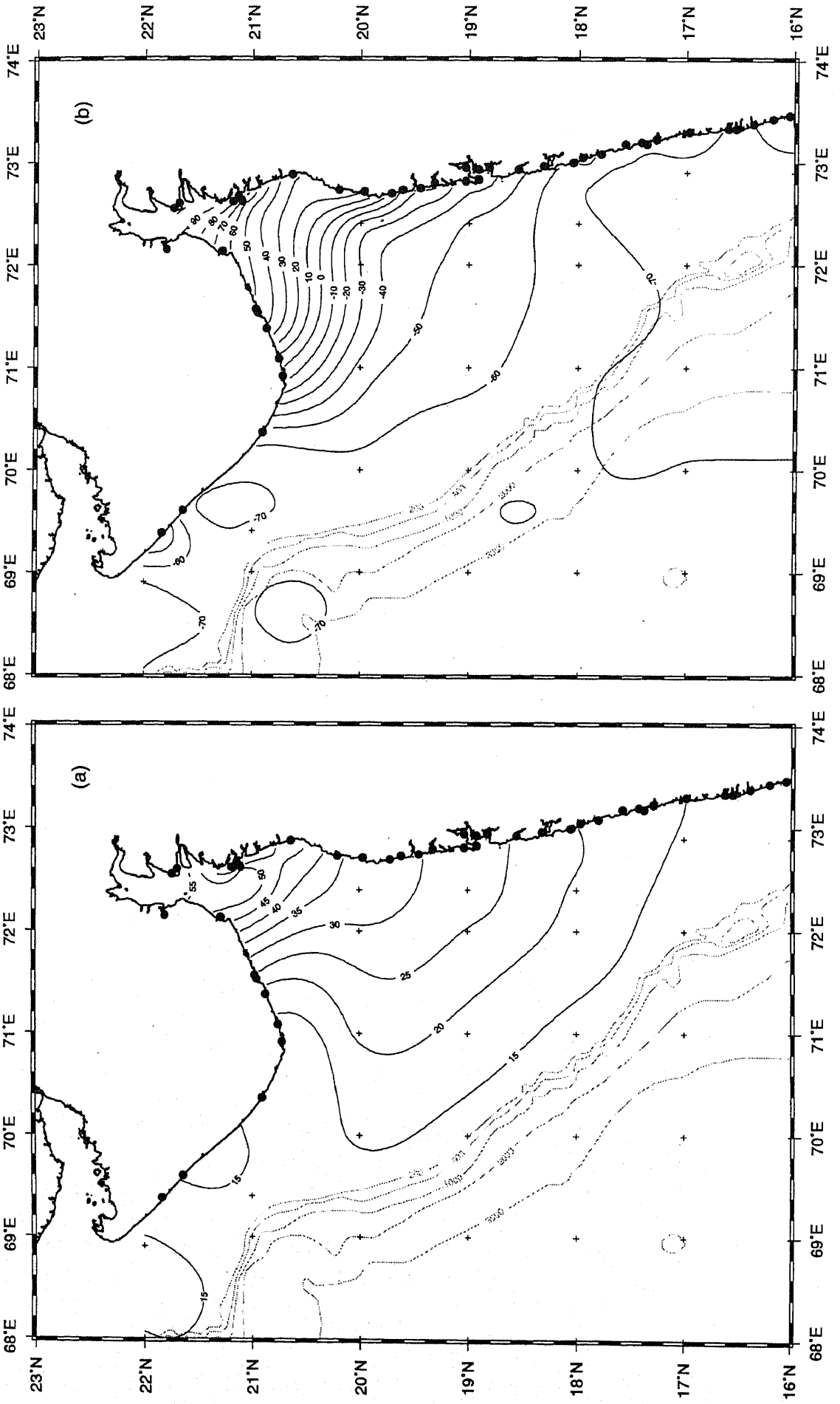

Figure 7. Same as figure 2, but for N_2.

This shelf region being more than 100 km wide and less than 200 m deep, the circulation here is expected to be dominated by shallow water processes, the components of which are tides, influence of local winds, and possibly influence of runoff from adjoining rivers. Another component of the circulation is expected to be the influence of large-scale wind-driven circulation. The northward seasonal coastal current along the west coast of India during the northeast monsoon is known to have its core located on the shelf break (Shetye *et al* 1991). It should be exerting at least some influence on the circulation on the shelf.

The state of knowledge of the circulation in the region is such that we do not have quantitative information on any of the components mentioned above. In the present study we make a beginning at addressing this issue by examining the contribution of tidal motion to the circulation. In particular, we address the following questions: What are the characteristics of tides in the region as seen in historical data? Can these characteristics be simulated in a numerical model? How do tidal currents simulated in such a model compare with observations? How important is the tidal circulation of the region in comparison to the large-scale wind-driven currents?

Tides along the west coast of India are mixed with the semi-diurnal constituents M_2 and S_2, and diurnal constituents K_1 and O_1 being the most prominent. Historical data on amplitudes and phases of these constituents are found in published literature at a number of ports in the region. In the next section we assemble these data to describe characteristics of propagation of tides in the region of interest. In section 3 we describe a barotropic nonlinear numerical model to simulate the tides in the region. The model predictions are compared with the observed tidal characteristics in section 4. The last section summarizes the results.

2. Data on tides

Historical data on tidal constants along the stretch of the west coast of India from Miani to Malvan, including the Gulf of Khambhat, is available in published literature at the forty-two stations shown in figure 1. These data have been reported in:

- Special Publications by the International Hydrographic Bureau (IHB), Monaco, published during the last few decades,
- Volume 2 of Admiralty Tide Tables (ATT, see, for example, the tables for 1998).

The number of constants covered in the latter are only four, M_2, S_2, K_1, and O_1. The IHB tables give a larger number of constants. Of the 42 stations, two – Pipavav and Suvali – have data on only the four constants found in the ATT. In the IHB data set, 7 constants are available at Sultanpur, 9 at Bhavnagar, 53 at Mumbai, and 60 at Veraval. At 36 stations the number of tidal constants varies between 28 and 38. The tidal constants at three stations, Porbandar, Veraval, and Mumbai (Apollo Bandar), have been computed from data collected during the period of one year, with the central time of the period in 1970, 1961 and 1952, respectively. The constants at one station, Port Albert Victor, which is close to the new port of Pipavav, are based on a 4 year long tidal record collected during 1900–1903. The constants at thirty-six stations have been computed from a month-long record each sometime during the period 1948–70.

The tidal constants from forty-two stations discussed above form our primary data set to describe the tides close to the coastline. We complement this set with a global data that has been described by Le Provost *et al* (1994). It was constructed using a finite element hydrodynamic model. The original intent behind constructing the model was prediction of tidal contribution to sea surface height variation measured by satellite altimeters. The model solution has been found to be reliable in the open ocean areas where the accuracy approaches that of tidal analysis methods (Le Provost *et al* 1995). The model performance is particularly good in the open North Indian Ocean (Le Provost *et al* 1994), and hence is a suitable choice to complement the coastal tidal data set.

The field of amplitude and phase of six most prominent tidal constituents in the region – M_2, K_1, S_2, O_1, P_1, and N_2 – are shown in figures 2–7. In plotting the contours shown in the figures we have given maximum weightage to those stations that are on the open coast and not in semi-enclosed areas such as creeks.

Table 1. *Amplitude and amplification factor for four locations – Jaigarh, Bombay, Ambheta, and Suvali – along the coast. The amplitude of the four major tidal constituents (M_2, S_2, K_1, and O_1) is given in cm. The amplification factor at a coastal station is given in brackets following with amplitude, and is defined as the ratio of amplitude at the station to that at the offshore edge of the model domain.*

	M_2 (cm)	S_2 (cm)	K_1 (cm)	O_1 (cm)
Offshore edge of model domain	53.9	20.6	31.0	15.9
Jaigarh	74.9 (1.4)	28.5 (1.4)	34.8 (1.0)	17.1 (1.1)
Bombay (Apollo Bandar)	123.0 (2.3)	48.0 (2.3)	42.0 (1.2)	20.0 (1.2)
Ambheta	270.0 (5.0)	76.1 (3.7)	62.7 (2.0)	32.5 (2.0)
Suvali	205.0 (3.8)	73.0 (3.7)	58.0 (1.9)	24.0 (1.5)

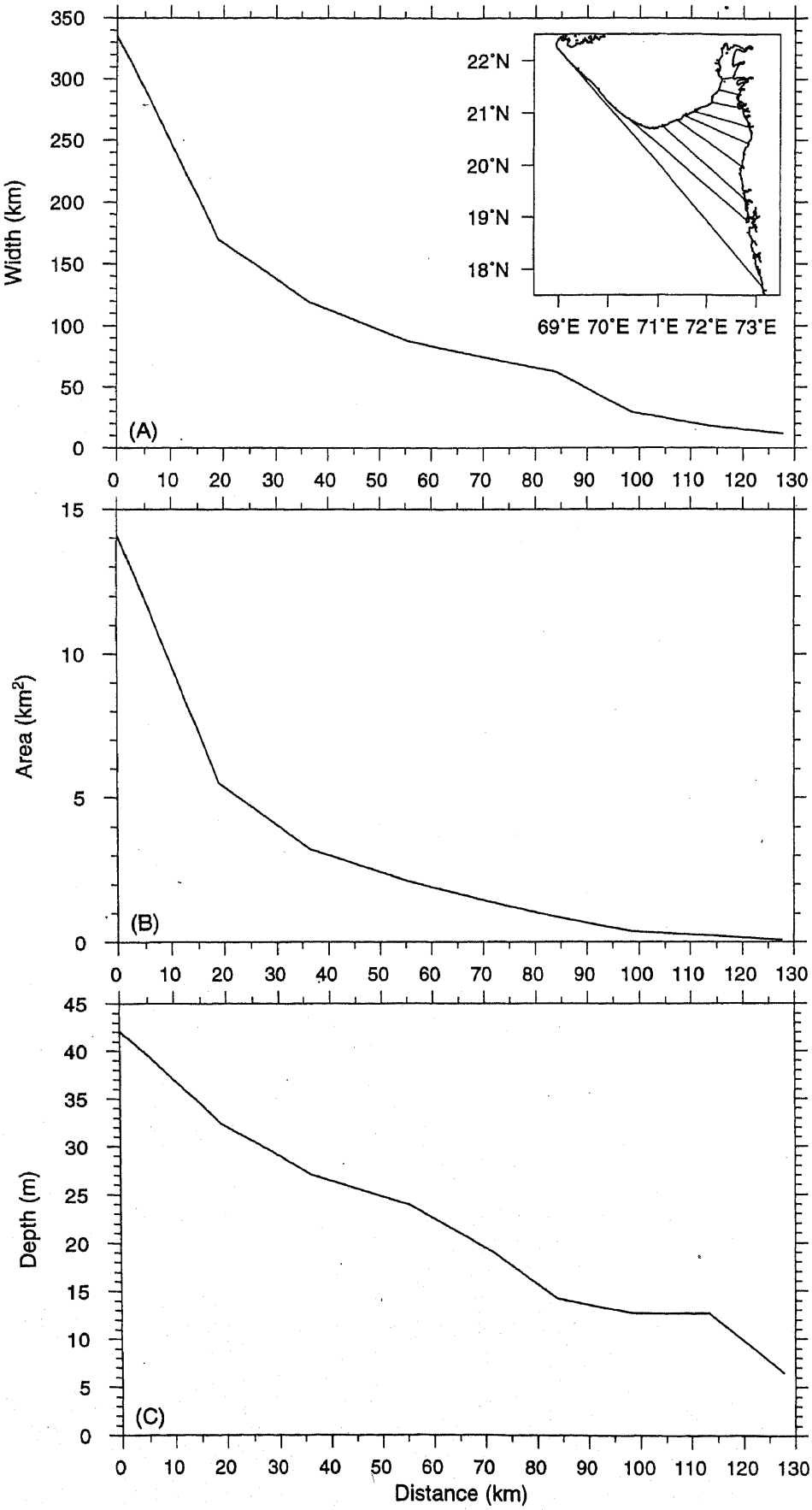

Figure 8. Simplified geometry of the Gulf of Khambhat and surrounding areas. (**A**) The variation in width (km) as measured at the 9 sections shown in the inset. Distance (km) is measured from the section farthest from the Gulf along the central line shown in the inset. (**B**) same as (A) but for cross-sectional area (sq. km); (**C**) same as (A) but for mean depth (m).

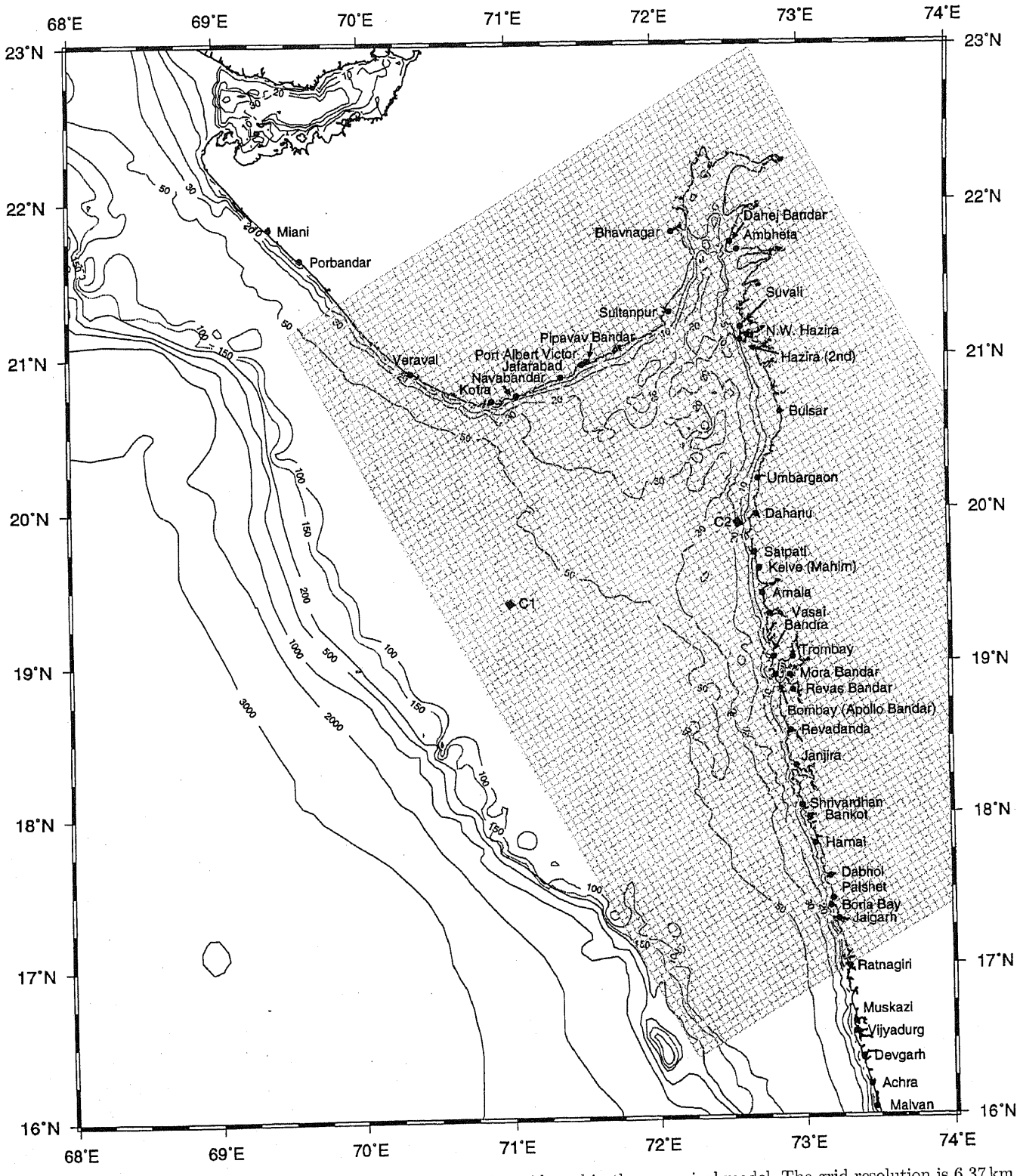

Figure 9. The model domain is shown by covering it with the grid used in the numerical model. The grid resolution is 6.37 km, along both axes. The grid axes are inclined at an angle of 30° in clockwise direction with east/north.

A sizable increase in amplitude can occur inside such creeks. The Bhavnagar station in the Gulf shows amplitudes that are much higher than those at other nearby stations. We believe that this is in part due to the location of this station inside a creek. Also, some stations in the shallow areas of the Gulf show noticeable decrease in amplitude. Dahej Bandar is an example. A possible cause of this is the marshy environment around the point where tidal measurements were made. Though the forty-two coastal stations provide a good description of how tidal constants vary along the open coast, they are insufficient to describe how the constants vary spatially at the upstream end of the Gulf of Khambhat.

In spite of these limitations, the data are sufficient to reveal major characteristics of tides in the region. The amplitude of each of the six constituents shown in figures 2–7 starts increasing as the tide propagates into the region where the shelf is noticeably wider than that to the north or south. The increase in amplitude accelerates as the tide moves into the funnel shaped region leading into the Gulf of Khambhat. Table 1 reveals some interesting characteristics of the amplification of diurnal and semi-diurnal tides as they propagate from the shelf break towards the coastline. The amplification factor (defined as ratio of amplitude at a coastal station to that at the shelf break) at Bombay is 2.3 for both the M_2 and S_2 tides; and 1.2 for K_1 and O_1. The ratio ranges between 3.5 and 5 for the semi-diurnal tides at Ambheta and Suvali, whereas for the diurnal tides the range is between 1.5 and 2.0. These two stations can be taken to represent the central part of the Gulf of Khambhat. This suggests that modification of the tide does not follow any simple rule, though the principal semi-diurnal constituents amplify much more than the diurnal ones. It is expected that the change in amplitude and phase as the tide propagates coastward is a function of geometric and frictional effects, the latter being highly non-linear.

From the following consideration we can appreciate the role of geometry in amplifying the tide. Consider a straight section along approximately the 50 m isobath, joining Dwarka (12°16′ N, 68°57′ E) to Dhabol as shown in figure 8. The section forms the open end of a funnel-shaped region that leads into the Gulf of Khambhat. Upstream of the section we have drawn other sections that lead progressively towards the narrow and shallow confined area at the upstream end of the Gulf (see the inset in figure 8(A)). These sections have been drawn approximately parallel to the lines of equal phase in the Gulf (figures 2–7). Hence, the average area, width, and depth of the sections represent the principal elements of the geometry felt by the tide as it propagates upstream into the Gulf. Figure 8(A, B and C) show, respectively, average width, cross-sectional area and depth as a function of distance from the open end of the funnel-shaped region. From these figures we note that the width of the region decreases exponentially, with e-folding distance of approximately 50 km, and the mean depth along each section decreases linearly towards the upstream end of the Gulf. As a result, the cross-sectional area decreases nearly exponentially with distance from the open end. The resulting confinement of the tide must lead to amplification. The extent of the amplification, however, is also dependent on frictional dissipation which is a non-linear function of velocity and depends on contribution to the velocity field from all tidal constituents (Le Provost and Fornerino 1985). In the next two sections we attempt to simulate the characteristics of tidal propagation into the gulf using a barotropic non-linear model so that the complicated interaction between the geometry, friction, etc. are properly accounted for.

3. Tidal model

Consider an undisturbed sea with depth h, a function of co-ordinates (x, y). Let motion lead to disturbance of the free surface by $\eta(x, y, t)$ and let (u, v) be the vertically averaged velocity over the water column of height $(h+\eta)$. The transport (U, V) is given by

$$U = u(h+\eta), \tag{1}$$

and

$$V = v(h+\eta). \tag{2}$$

The momentum and continuity equations can then be written as,

$$\frac{\partial U}{\partial t} + \frac{\partial}{\partial x}(uU) + \frac{\partial}{\partial y}(vU) = -g(h+\eta)\frac{\partial \eta}{\partial x} + fV + A_H\nabla^2 U - C_D\frac{U\sqrt{U^2+V^2}}{(h+\eta)^2}, \tag{3}$$

$$\frac{\partial V}{\partial t} + \frac{\partial}{\partial x}(uV) + \frac{\partial}{\partial y}(vV) = -g(h+\eta)\frac{\partial \eta}{\partial y} - fU + A_H\nabla^2 V - C_D\frac{V\sqrt{U^2+V^2}}{(h+\eta)^2}, \tag{4}$$

and,

$$\frac{\partial \eta}{\partial t} + \frac{\partial U}{\partial x} + \frac{\partial V}{\partial y} = 0, \tag{5}$$

where t, g, f, A_H, and C_D are respectively time, acceleration due to gravity, Coriolis parameter, coefficient of horizontal diffusion of momentum, and bottom drag coefficient. We solve these equations under the condition that η at the open boundaries of the sea behaves in a prescribed manner. We shall define η along these boundaries using the output of the global tidal model described in Le Provost *et al* (1994) and discussed in the previous section.

The domain of the model is shown in figure 9. Equations (1)–(5) were solved numerically using a finite difference Arakawa-C grid, and a leap-frog technique to march in time. The parameters used in the model are summarized in Table 2. A no-slip condition was imposed along the solid boundaries. The tide at the intersection of two straight open boundaries, i.e. at the northwest and southwest corners of the rectangular domain, was defined using the output of the global

Table 2. *Parameters used in the numerical model.*

$\Delta x, \Delta y$	6.37 km
Δt	36 sec
C_D	= 0.01 if $h \geq 70$ m = 0.004 if 25 m $\leq h <$ 70 m = 0.0015 if $h \leq 25$ m
A_H	5000 $m^2 s^{-1}$
f	4.72×10^{-5} sec^{-1}

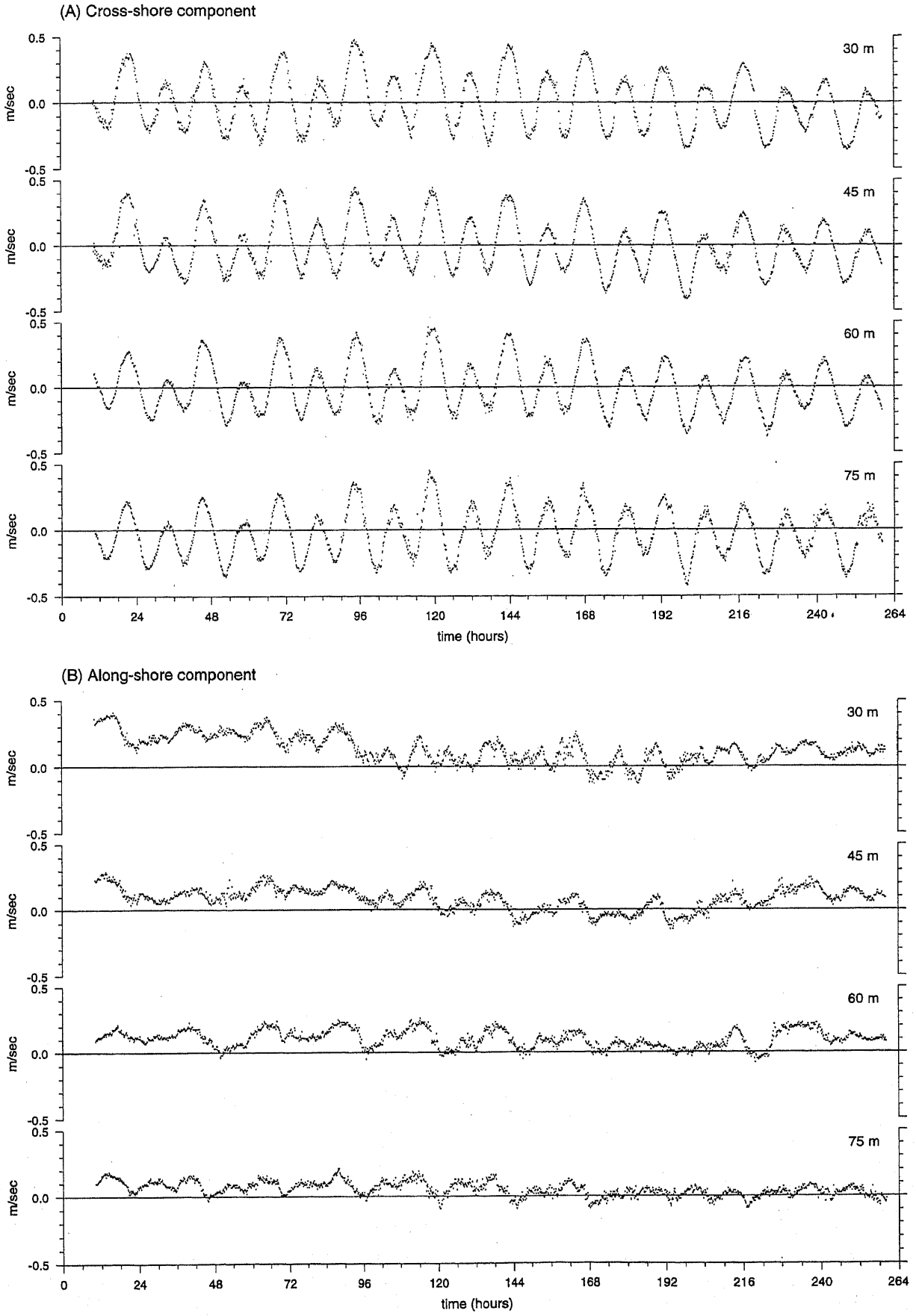

Figure 10. Currents (m/sec) observed at (19° 24.5′N and 71° 2.5′E) in the Bombay High region during 24th December 1981 – 3rd January 1982 (see Fernandes *et al* 1993). Zero hour along the time-axis is 0000 hours on 23rd December 1981. The currents were measured at four depths: 30, 45, 60 and 75 m; the total depth at the location is 80 m. (**A**) The component along the x-axis (cross-shore axis) of the model grid shown in figure 9. (**B**) The component along the y-axis (along-shore axis) of the model grid.

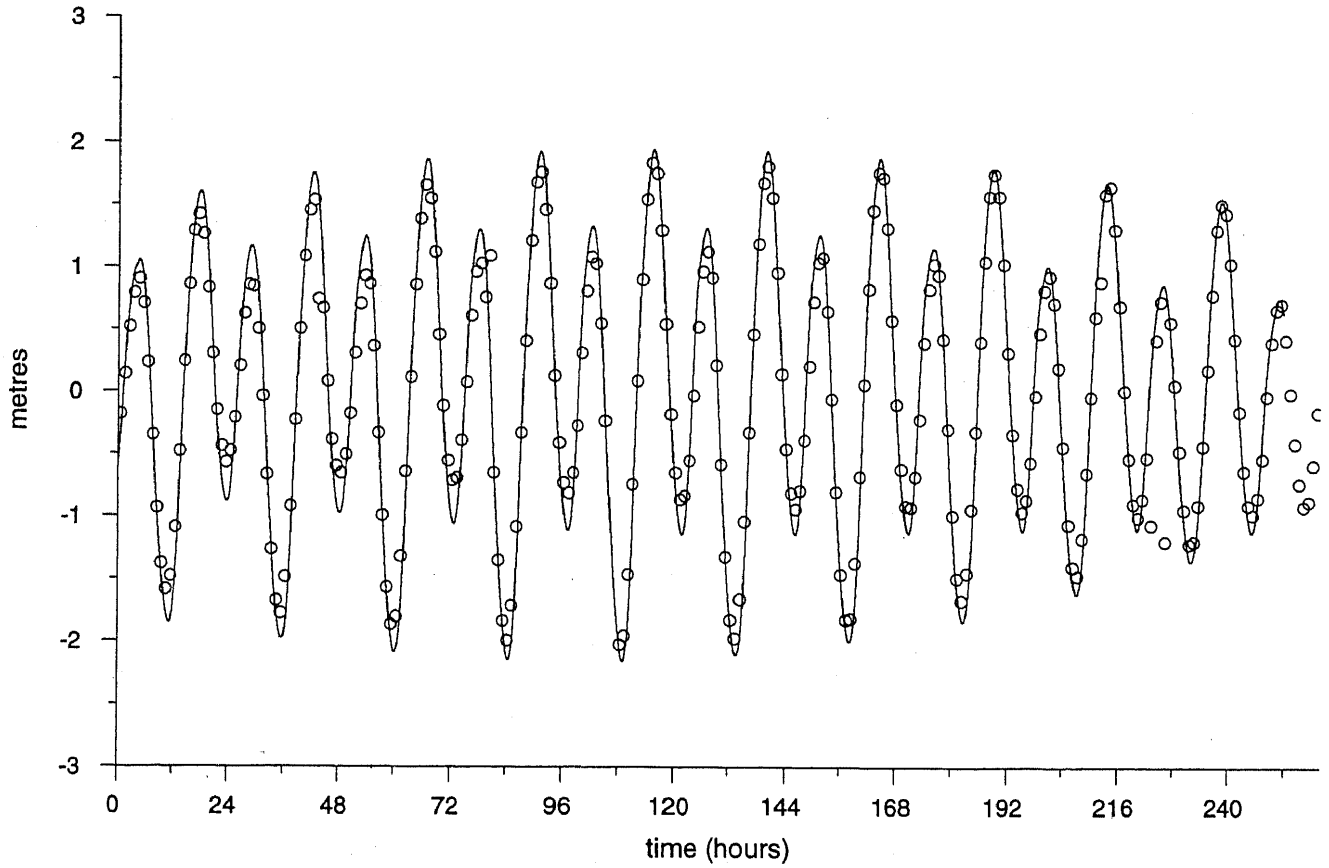

Figure 11. Comparison between hourly sea level (m) observed (open circles) at Bombay (Apollo Bandar) and the sea level predicted (continuous line) by the model during 24th December 1981– 3rd January 1982. Zero hour along the time-axis corresponds to 0000 hours on 23rd December 1981.

tidal model discussed in the previous section. The tide at the remaining two corners was constructed by making a prediction based on the constituents at the coastal stations. The method of prediction follows that of Glenn (1977). In this method, a total of 25 constituents are considered for prediction, using the amplitudes and phases of four major constituents and taking the remaining by admittance. The tide at grid-points between any two corners was defined by a linear interpolation using the values at the two corners.

In a typical run, the model was forced with a composite tide along the open boundaries and was spun up within approximately 5 days. It was then run for another month, and the model output during this period was used to analyze the model performance. Harmonic analysis was carried out to determine characteristics of the major constituents, M_2, S_2, K_1 and O_1. To compare simulated currents with observations, model runs were also made for the period when current meter data are available.

4. Model results

We present model results in three different ways. First, we compare predicted tidal heights and currents with the observations available in the region. Second, we compare tidal amplitudes and phases computed from the model with those observed in the coastal tidal data set. Finally, we present simulated tidal currents during a typical tidal cycle.

4.1 *Sea level and currents*

Reports of sea level and direct current measurements in the region are very few. Tide gauge record is available from Bombay (Apollo Bandar). Direct current meter observations are very rare. The two records we have had access to, one at Bombay High and the other off the port at Dahanu, each cover a period of about a week. Below we compare the predicted sea level at Bombay with the tide-gauge record at Apollo Bandar during the week-long period when the time series of currents is available at Bombay High. We then compare predicted currents at Dahanu with observations.

Fernandes *et al* (1993) reported direct current meter observations at the location (19° 24.5′ N and 71° 2.5′ E) in the Bombay High region. At this location, the depth is 80 m and measurements were made at four depths (30, 45, 60 and 75 m) during the period from 24-12-1981 to 2-1-1982. Figure 10 shows these currents. As

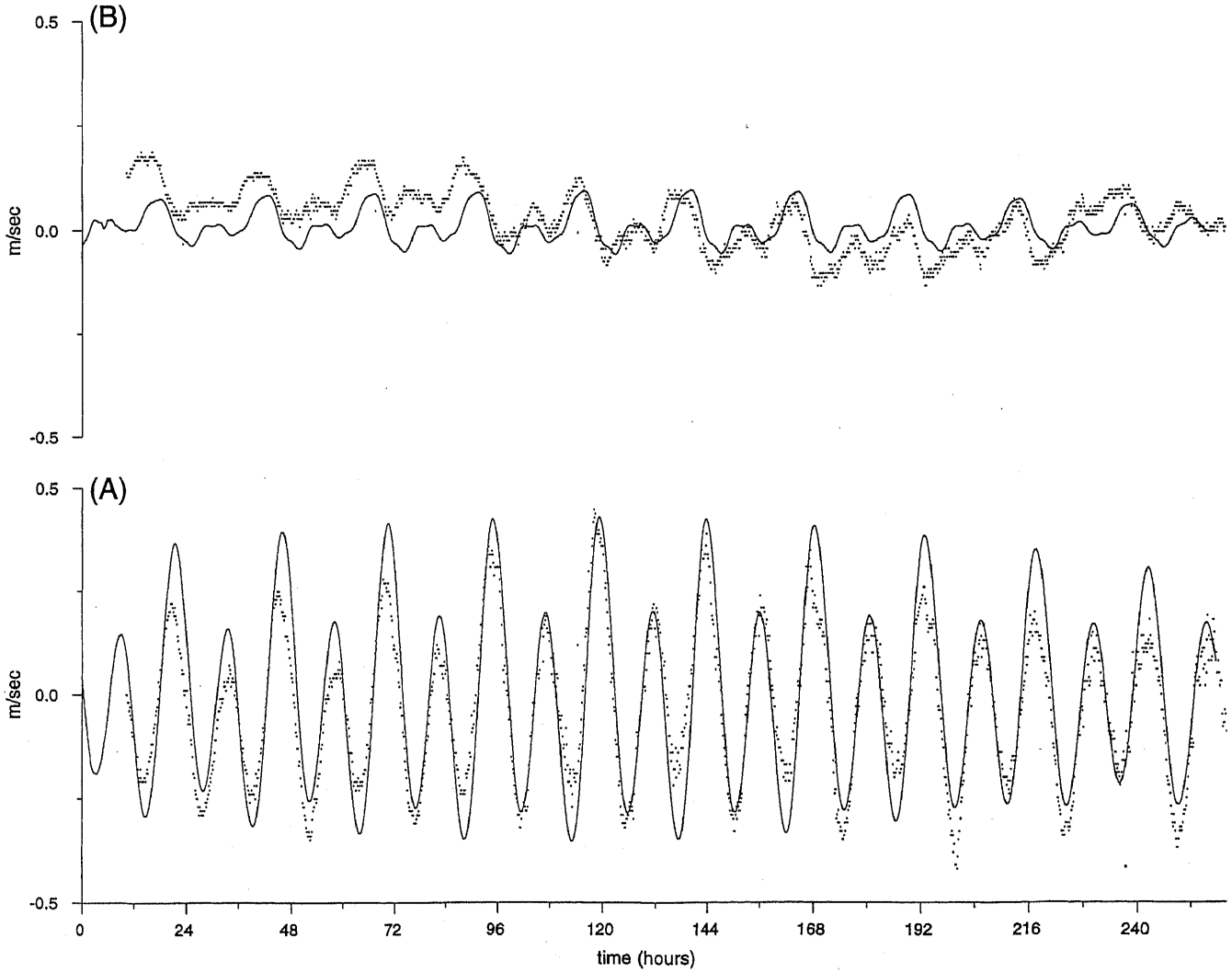

Figure 12. Comparison between the vertically-averaged currents (m/sec) observed (open circles) at Bombay High and the currents predicted (continuous line) by the model during 24th December 1981 – 3rd January 1982. Zero hour along the time-axis corresponds to 0000 hours on 23rd December 1981. The currents were computed by averaging those shown in figure 10. (**A**) The component along the x-axis (cross-shore axis) of the model grid shown in figure 9. (**B**) The component along the y-axis (along-shore axis) of the model grid.

seen in the figure, the currents have distinct variability at semi-diurnal and diurnal periods, suggesting that the currents are mainly tidally-driven. No noticeable variation with depth is seen, suggesting that they are predominantly barotropic. This is consistent with the formulation of the model.

We have used the tide gauge record from Apollo Bandar for the same duration as the current meter record to compare the predicted sea level with observations (figure 11). As seen from the figure, the comparison is favourable. Both the amplitude and the phase are reproduced well.

Figure 12 shows the vertically averaged eastward and northward component of the current computed from the Bombay High current meter record. In this figure we have also plotted the currents predicted by the model. As seen from the figure, the comparison is favourable but there are some differences. The predicted component of the onshore-offshore component (u-component) matches very well with the observed component (figure 12 (A)). But, there are systematic differences in the alongshore component (v-component) as seen in figure 12(B). The observed alongshore current has a mean flow directed towards the north during the first half of the period of observations. We believe that the northward current is a signature of the seasonal large-scale wind-driven current that is known to occur along this coast (Shetye *et al* 1991). Its core is located on the continental slope and the current is best developed during the northeast monsoon. Figure 12(B) then suggests that the coastal current does influence, though marginally, the tidally-dominated flow on the shelf.

The current meter record off the port of Dahanu was collected in much shallower depth, about 15 meters, during February 24th – March 3rd, 1996. Once

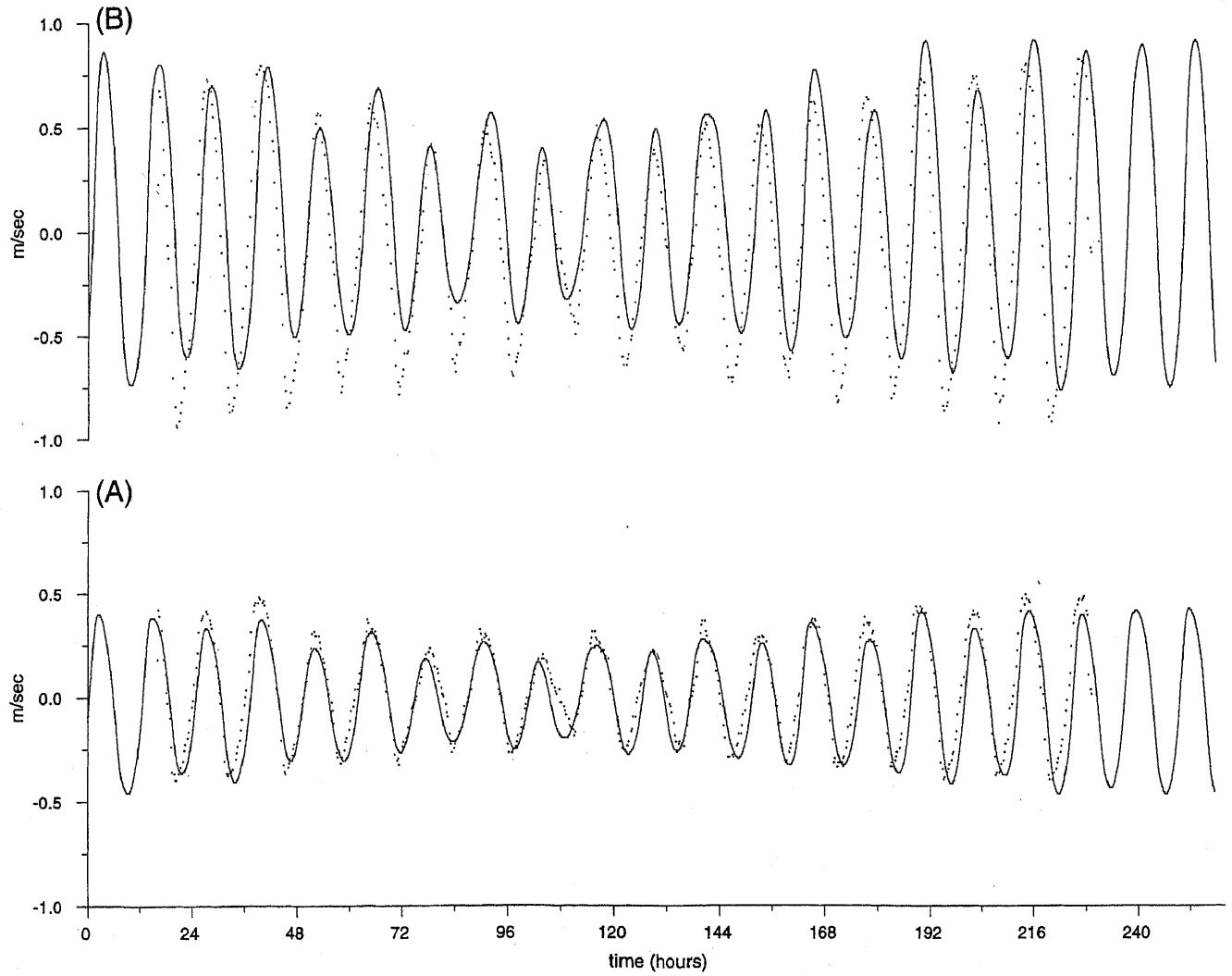

Figure 13. Comparison between currents (m/sec) observed (open circles) at a location off the port of Dahanu and the currents predicted (continuous line) by the model during 24th February – 3rd March 1996. Zero hour along the time-axis corresponds to 0000 hours on 24th February 1996. (**A**) The component along the x-axis (cross-shore axis) of the model grid shown in figure 9. (**B**) The component along the y-axis (along-shore axis) of the model grid.

again, we find from figure 13 that the observations and the model predictions are in good agreement.

4.2 *Amplitudes and phases of tidal constituents*

Harmonic constants from 32 stations that fall within the model domain (figure 9) were used in comparing the model output with observed amplitudes. Actually there are 33 stations that fall in the model domain. Of these there are two at Hazira. Only one of these, N.W. Hazira, was used in the comparison. The model output from those grid points that correspond most closely to the 32 stations were used. The model sea surface elevations from a one month-long run were subjected to harmonic analysis using the TASK package of the Proudman Oceanographic Laboratory, U.K. (Anonymous, 1996) to determine amplitudes and phases. In figures 14 and 15 we compare the model computed and the observed amplitudes and phases.

From the figures it can be seen that the most important semi-diurnal tides, M_2 and S_2, are modelled the best and, except for some outliers, the predicted amplitude and phase compare favourably. In the figures we have identified these outliers. Bhavnagar is one. As pointed out earlier, this station is located inside a creek, and its amplification appears to be strongly influenced by conditions in its immediate vicinity. The resolution used in our model could not have resolved these conditions adequately. Some other stations also stand out as outliers: Dahej Bandar and Ambheta, for example. Both are located near the upstream end of the Gulf of Khambhat, and here too we expect that the model resolution is too coarse to achieve a precise match with the observations.

The diurnal species, O_1 and K_1, that have amplitudes weaker than those of the semi-diurnal M_2 and S_2 species, are not simulated as well as the latter. The number of outliers in the case of the diurnal

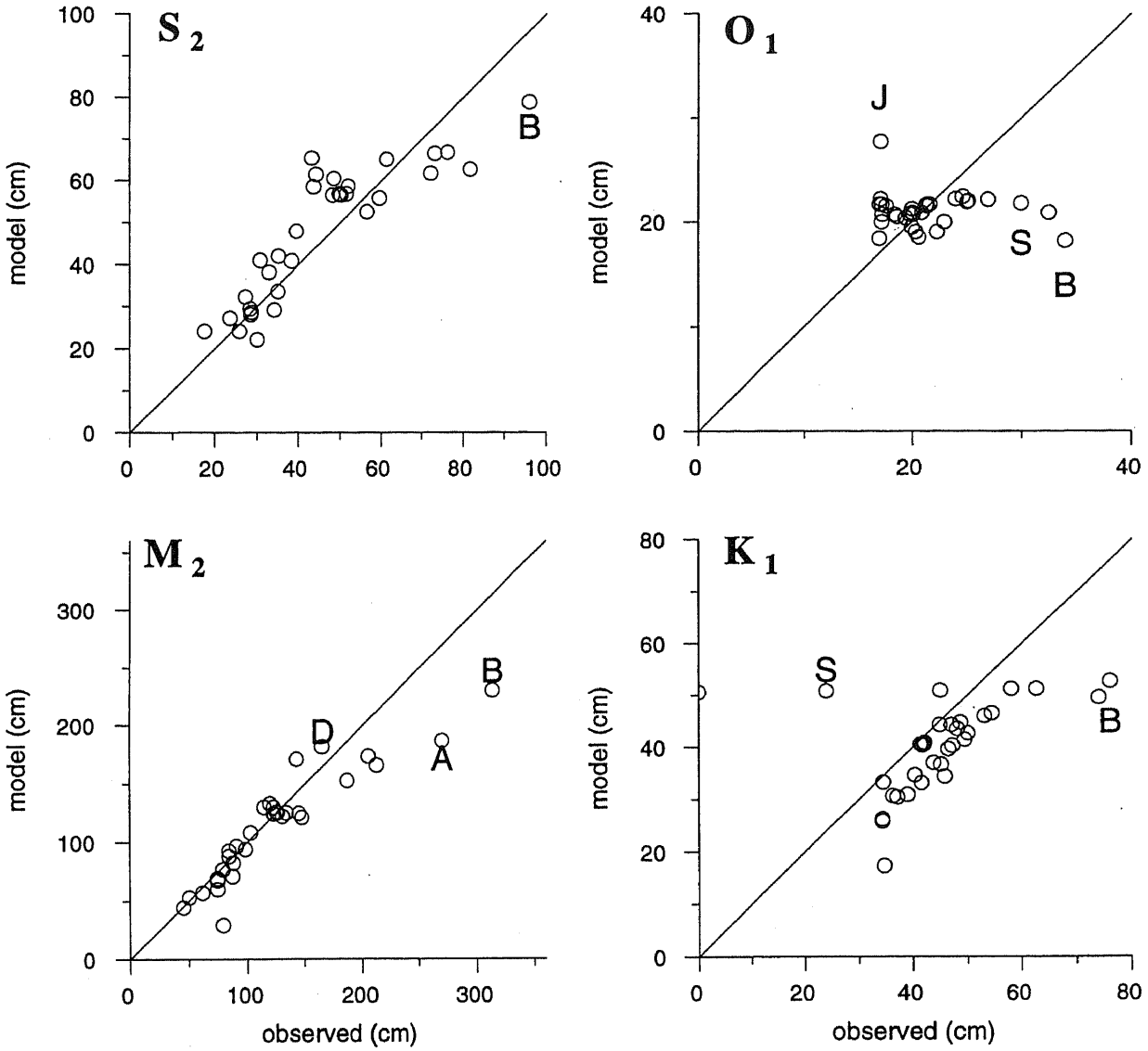

Figure 14. Comparison between amplitude (cm) of M_2, S_2, K_1, and O_1 tidal constituents computed from observations and those computed from model predictions. The letters identify those locations where the two amplitudes do not match very well: Dahej Bandar (**D**), Bhavnagar (**B**), Ambheta (**A**), Suvali (**S**), Sultanpur (**Su**), and Jaigarh (**J**).

constituents is larger. This is consistent with the experience of tidal numerical models elsewhere in the world: as the amplitude decreases, ability of the model to simulate those constituents deteriorates. One reason for this is that the non-linear friction term in the model can act either as a source or as a sink of energy depending on correlation between velocities corresponding to different tidal constituents (Le Provost and Fornerino 1985). The problems arising from such issues are generally handled by tuning the drag coefficient in the model. We have not attempted this because our primary interest was in demonstrating the feasibility of simulating the tidal currents reasonably well to be useful in environmental management. We do seem to have succeeded in meeting this objective. Moreover the model does offer the promise that higher spatial resolution and finer tuning of friction coefficients can further improve the model performance.

4.3 *Circulation during a typical tidal cycle*

Figure 16(A–D) summarizes the evolution of currents during a typical spring tide semi-diurnal cycle. Figure 16(A) shows the velocity field when it is high tide at Bombay. The remaining three figures show how the velocity field changes as the sea level at Bombay goes from a maximum to a minimum and then back to a maximum. The figures show how the currents change as the tide propagates over the wide shelf and in and out of the Gulf of Khambhat.

5. Concluding comments

In this paper we have shown that it is feasible to simulate reasonably realistically tidal currents in the Bombay High and surrounding areas including the

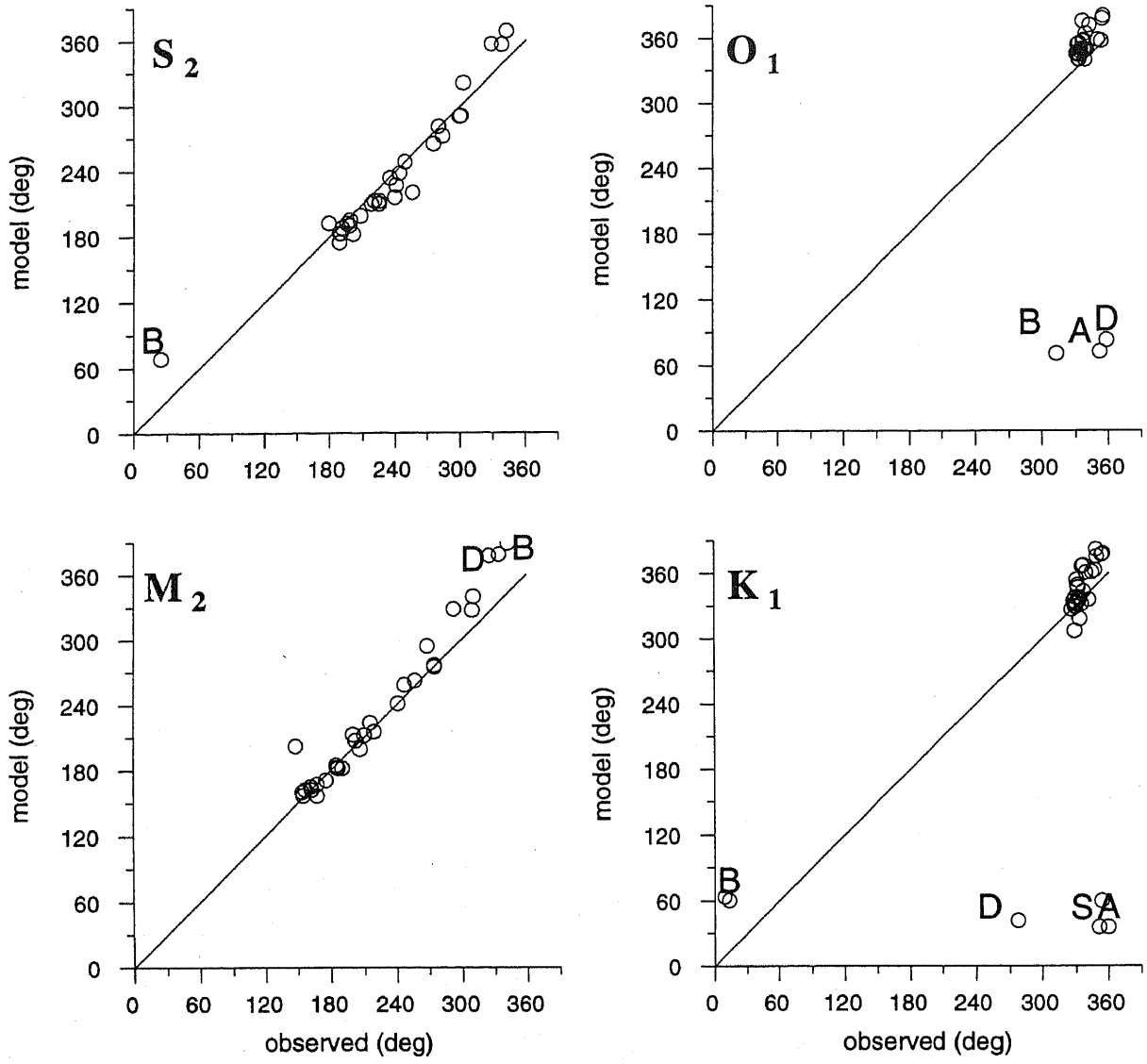

Figure 15. Same as figure 14 but for phase in degrees.

Gulf of Khambhat using a barotropic model. As pointed out in section 1, this area is of interest for many practical reasons, and the study of tides is a first step towards the understanding of oceanography of the region. The results reported here further suggest that with a finer resolution and tuning of frictional drag coefficients, currents could be modelled with even better accuracy than what has been achieved now. Though the success of the model is encouraging, a few limitations in checking the model performance need to be noted.

First, the data base on direct current observations in the region is weak. The absence of time-series longer than a week, makes it difficult to separate tidal currents from wind-driven low-frequency currents. In section 4.1 we noted possible signatures of the poleward seasonal northeast monsoon coastal current in the observations at Bombay High. This current arises from the large-scale wind field over the north Indian Ocean. It is quite possible that during the southwest monsoon the shelf experiences effects arising from other driving functions. The runoff in the Gulf of Khambhat and surrounding areas is one possible driving mechanism. We are not in a position to examine these possibilities due to the lack of an appropriate database.

Second, our understanding of the hydrography of the region is poor. For example, we do not know the characteristics of stratification in the region. Using a rare direct current meter record available in the Bombay High region we have inferred that the currents are essentially barotropic. This may well be the case during the northeast monsoon. But, during the southwest monsoon, precipitation and runoff could build sufficient stratification to make baroclinicity important. Absence of information on hydrography of the region prevents us from appreciating the contribution of baroclinicity to the circulation in the region.

We are therefore led to the conclusion that further progress in realistic simulation of the currents will be

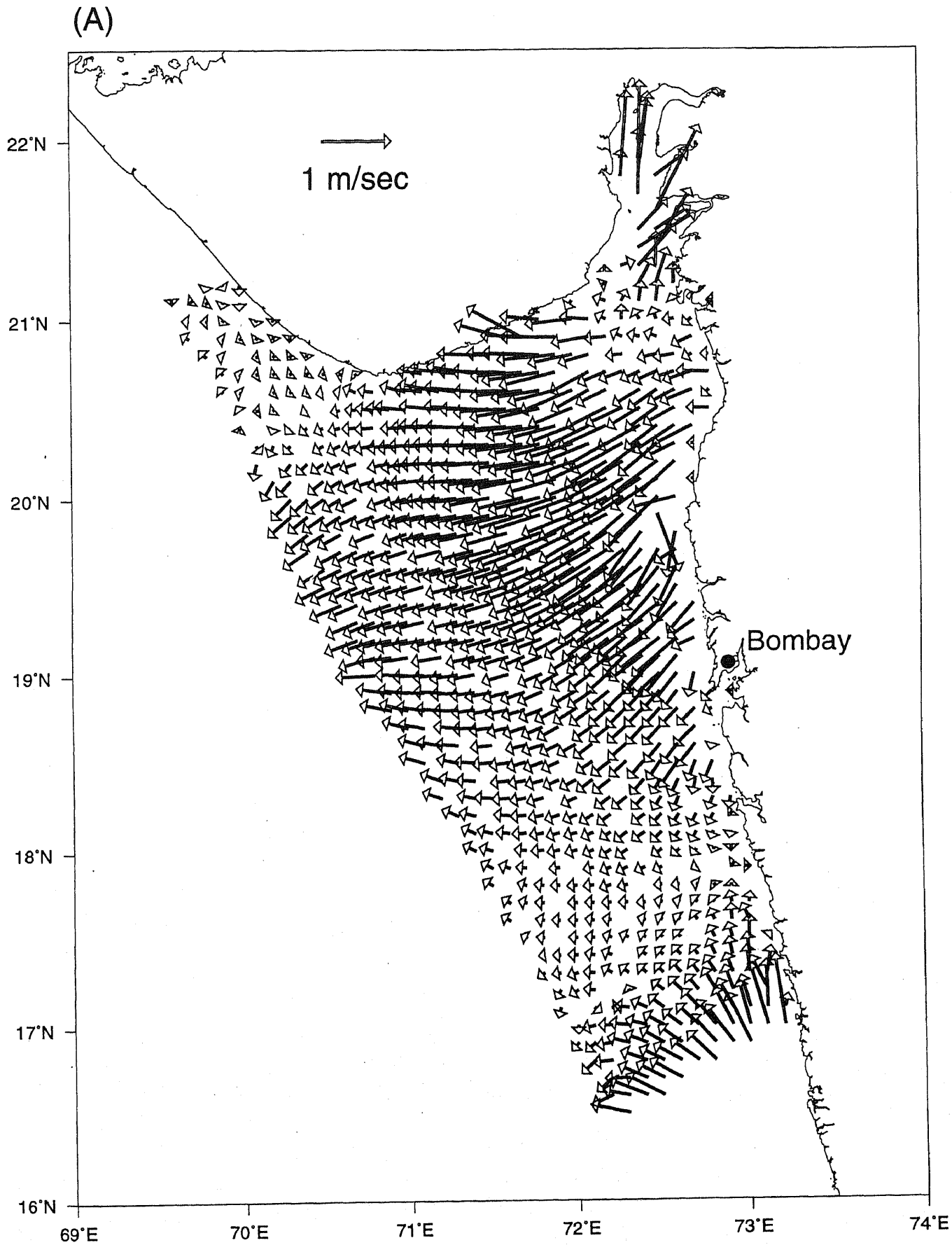

Figure 16(A). (*Continued*)

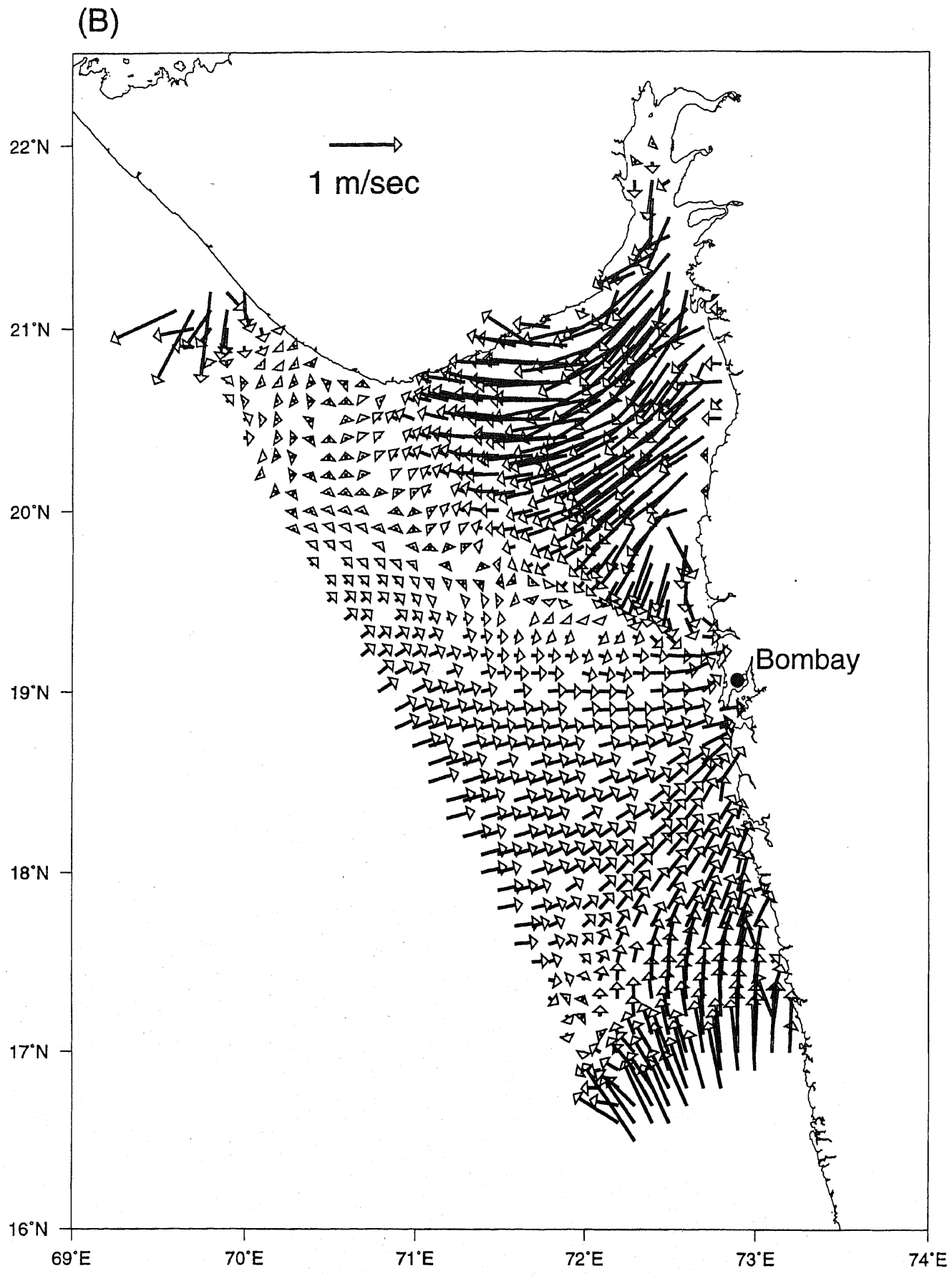

Figure 16(B). (*Continued*)

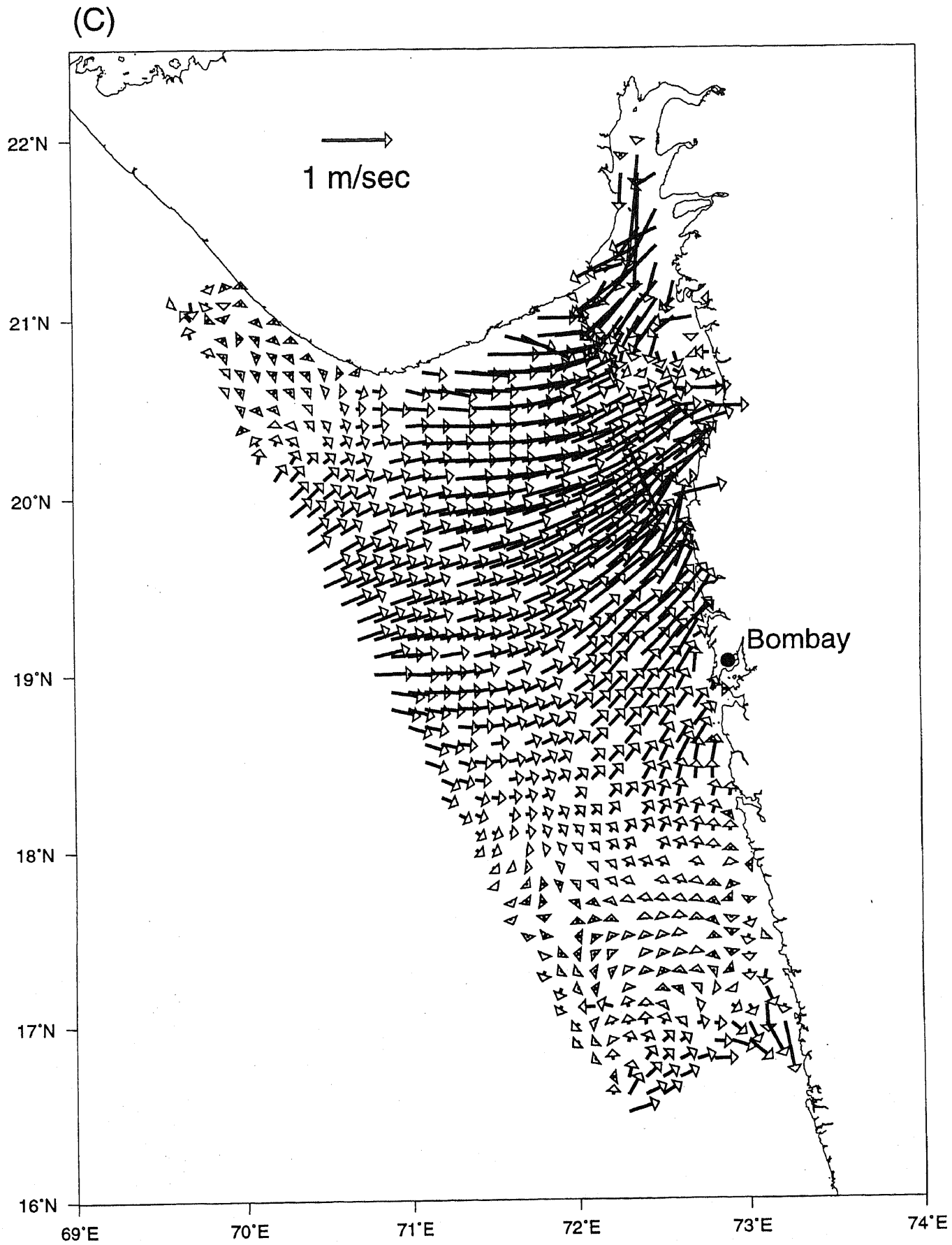

Figure 16(C). (*Continued*)

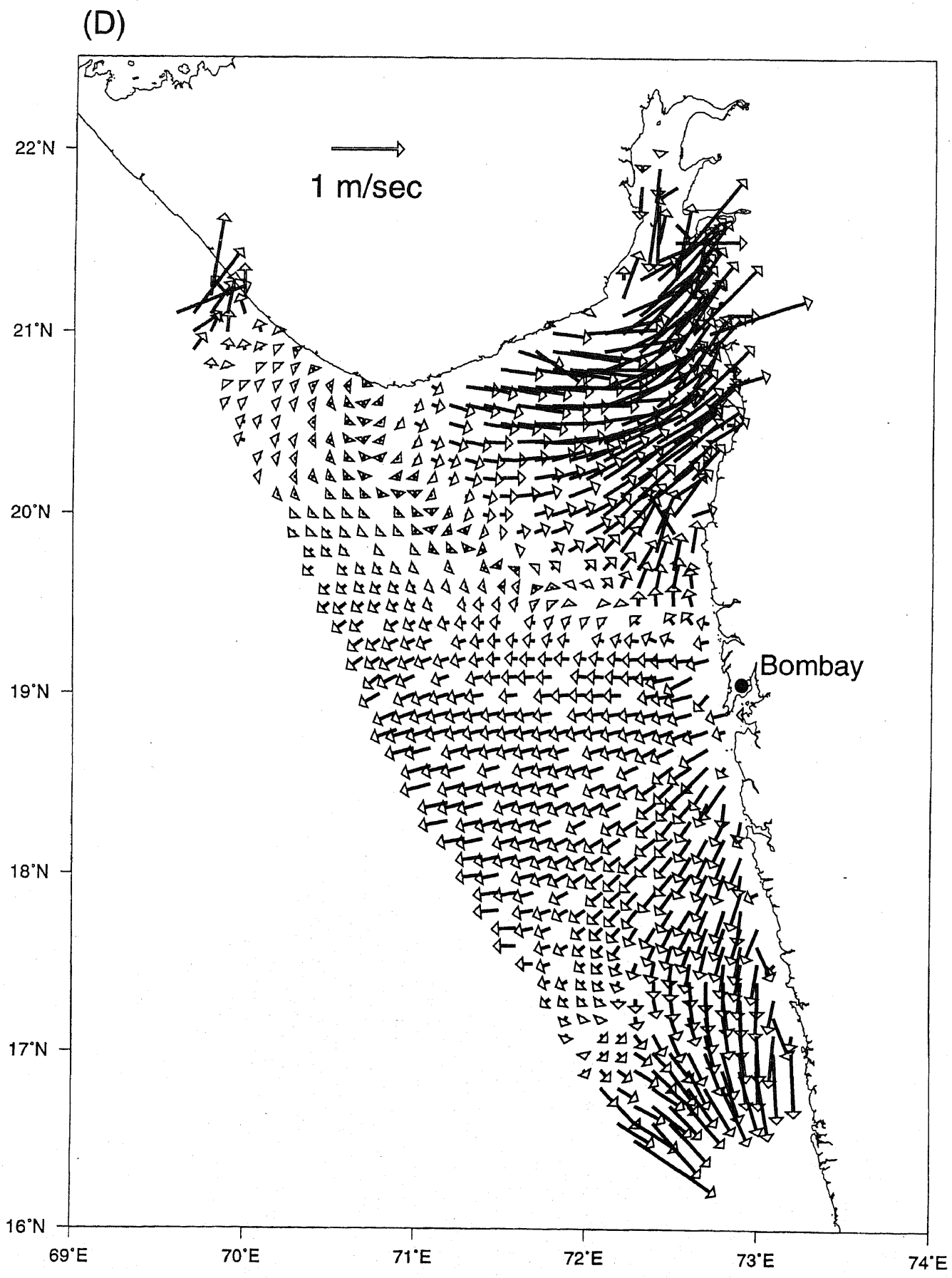

Figure 16. Typical cycle of velocity field during a tidal cycle; (**A**) velocity field when it is high tide at Bombay. (**B**) Mid-way to low tide; (**C**) Low tide; (**D**) Mid-way to high tide.

critically dependent on the availability of improved observational databases.

Acknowledgements

The present work forms a part of a grant-aid-project funded by the Department of Ocean Development, Government of India (NIO Contribution No. 2663).

References

Admiralty Tide Tables, Vol. 2, 1996 Published by the Hydrographer of the Navy, U.K.

Anonymous 1996 TASK: Tidal analysis Softaware Kit, Proudman Oceanographic Laboratory, Bidston, U.K., 15 pp.

Glenn R N 1977 The admiralty method of tidal prediction, np 159; *Int. Hydrogr. Review, Monaco* **52(2)** 431–450

Fernandes A A, Chandramohan P and Nayak B U 1993 Observed currents at Bombay High during a winter; *Mahasagar* **26(2)** 95–104

International Hydrographic Bureau 1930 *Tides, Harmonic Constants*: International Hydrographic Bureau, Special Publication No. 26 and addenda.

Le Provost C and Fornerino M 1985 Tidal spectroscopy of the English channel with a numerical model; *J. Phys. Oceanogr.* **15(8)** 1009–1031

Le Provost C, Genco M L, Lyard F and Vincent P 1994 Spectroscopy of the world ocean tides from a finite element hydrodynamic model. *J. Geophys. Res.* **99** 24,777–24,797

Le Provost C, Bennet A F and Cartwright D E 1995 Ocean tides for and from TOPEX/POSEIDON; *Science* **267** 639–642

Shetye, S R, Gouveia A D, Shenoi S S C, Michael G S, Sundar D, Almeida A M and Santhanam K 1991 The coastal current off western India during the north-east monsoon; *Deep-Sea Res.* **38** 1517–1529

MS received 1999 February 20; revised 1999 August 10